Fault tolerance in robotics

Farid Noureddine, Benoît Larroque, Frédéric Rotella

Fault tolerance in robotics

Farid Noureddine*, Benoît Larroque
and Frédéric Rotella

Laboratoire Génie de Production,
Ecole Nationale d'Ingénieurs de Tarbes,
47, avenue d'Azereix 65000 Tarbes, France
Fax: +33562442727
E-mail: farid.noureddine@enit.fr
E-mail: benoit.larroque@enit.fr
E-mail: rotella@enit.fr
*Corresponding author

Abstract: This work is a contribution to illustrate the fault tolerance concepts in robotics. Every step from the analysis phase to the fault accommodation phase is presented. A fault on joint 3 is taken into account and simulated to validate the detection algorithms. The fault accommodation is thus considered and is based on the kinematic redundancy principle. The establishment of the inverse kinematic model, under some conditions of joint failure, enables the generation of an alternative trajectory to ensure the robot goes on functioning.

Keywords: fault tolerance in robotics; fault tolerant robot manipulators; fault analysis; fault detection and isolation; methods based fault detection; fault accommodation.

Reference to this paper should be made as follows: Noureddine, F., Larroque, B. and Rotella, F. (2009) 'Fault tolerance in robotics', *Int. J. Mechatronics and Manufacturing Systems*, Vol. 2, No. 3, pp.294–310.

Biographical notes: Farid Noureddine received the PhD Degree in Robotics from the "Institut National des Sciences Appliquées de Rennes", France in 1987. He then worked for three years as Assistant Professor at the University of Sciences and Technology in Oran, Algeria, where he contributed to the creation of a Research Laboratory in Robotics. He directed this Laboratory for two years. In 1990, he joined the "Ecole Nationale d'Ingénieurs de Tarbes", France, where he is currently Assistant Professor. His main research interest lies in the model based fault detection isolation and especially in the field of robotics.

Benoît Larroque received PhD Degree in Automatic from the "Ecole Nationale d'Ingénieurs", (ENIT), Tarbes, France. He received the Diploma in Engineering from the "Ecole Nationale d'Ingénieurs", (ENIT), Tarbes, France, in 2004. His research focuses on observers design for Linear Time Invarying (LTI) and extends his work to the design of observers applied to linear time varying systems. The main field of application of his work is for Fault Detection and Isolation (FDI) problems applied for LTI and LTV systems. He worked as an Assistant Professor from 2004 to 2007 at the ENIT and from 2007 to 2008 at the "Université de Pau des Pays de l'Adour".

Frédéric Rotella received the Diploma in Engineering from the "Institut Industriel du Nord", Lille, France. He received the PhD and Doctorat d'Etat Degrees from the University of Science and Technology, Lille- Flandres- Artois, France, in 1983 and 1987, respectively. From 1981 to 1994, he was with the Laboratoire d'Automatique et d'Informatique Industrielle, Lille, where his research interests focused on modelisation and control of nonlinear systems. During this period, he served at the Ecole Centrale de Lille (ex. Institut Industriel du Nord) as Assistant Professor in Automatic Control. In 1994, he joined the Ecole Nationale d'Ingénieurs, (ENIT), Tarbes, France, as Professor of Automatic Control.

1 Introduction

If the favourite field of fault tolerance in robotics remains applications belonging to remote environments such as in space exploration or unstructured underwater environments (Sarkar et al., 2002), the fact is that some capabilities of fault tolerance would be equally appreciated in the industrial field. In fact, in some cases, if one of the parts of the robot were to fail, the reduced robot, thanks to some modifications, should still be capable of accomplishing the mission objectives. This capacity of coping with a fault on the robot enables to start a maintenance procedure as quickly as possible, without the emergency aspect involved by stopping the production. Such an operation implies that the robot is necessarily redundant in its normal mode as it can continue working despite a fault. As mentioned in Chen et al. (2003) it is worth noticing that some degrees of freedom are more important than others. Standard for robotics is often the 6 joints robot that allows a positioning and orientation in the dimensional Cartesian space, but there are also some task situations in an industrial context where less joints are required.

Note that in Paredis et al. (1994) it is shown that if one joint fails, a 9 degree-of-freedom manipulator must be designed to be fault tolerant and thus to respect a task of reaching a set of positions/orientations in the space. Having said this, it is hardly to be expected that a manufacturer purchases a 9 ddl robot, that is to say a special machine, to cope with one of its joints fault.

Since the 1990s a lot of works have been written about fault tolerance in robotics. In Visinsky et al. (1994), a survey has been proposed, all the necessary stages for designing a fault tolerant robot manipulator have been listed. A great attention has been devoted to present the tools used in the reliability analysis. This work has been completed by Visinsky et al. (1995) where the fault detection stage is based on the concept of analytical redundancy (Chow and Willsky, 1984). This last method is one of the three standards used in the fault detection methods for dynamic systems, the two others are based on the parameters estimation (Isermann, 1997) and the state estimation (Patton and Chen, 1997). Our work is based on this last method.

In English and Maciejewski (2000) joint failures are characterised in sense where data are defined in the Cartesian space by measuring a failure effect in this space. This work has been preceded by contributions in the field of redundant manipulators for locked joint failures. Paredis et al. (1994) showed that for a specific task a number of joints can be duplicated to attribute the property of fault tolerance to a robot

manipulator. He proposed a formulation of this problem and proofs of existence of robot manipulators are given by considering the duality between the number of actuators and tasks.

To complete this review of the existing works, let us quote two recent papers on fault tolerance in the designing of parallel robot manipulators (Hassan and Notash, 2007) and on an omnidirectional walking of legged robots with a failed leg (Yang, 2008). This later surveys all the necessary stages for defining a fault tolerant rigid-link-robot with closed-loop feedback control.

The considered robot in this paper is a five rotary-jointed robot, shown in Figure 1. Although most of the described procedures can be adapted to other types of robots, some designing procedures are dedicated to this robot, especially the proposed fault accommodation. Section 2 gives a review of a Failure Mode and Effects Analysis (FMEA). This is a qualitative method which determines the critical failure modes in system design. The third section treats of dynamic modelling which allows a fault dynamic analysis and contributes to set some diagnosis elements. The next section deals with the state space control on the one hand where the dynamic model of the robot is linearised around an operating point and on the other hand the implementation of the Fault Detection Isolation (FDI) stage. The fifth and last section describes the fault accommodation procedure.

Figure 1 A five rotary joints robot manipulator

2 FMEA

Analysing potential failures systems is a very important step to improve the system reliability. Applying standard approaches such as an FMEA (Noureddine, 1996), Fault Tree Analysis (FTA) or Failure Mode, Effects, and Critical Analysis (FMCEA) are often synonymous with efficiency and rigour. We therefore have chosen FMEA to carry out the considered robot analysis.

FMEA is a qualitative method used to identify potential failures of a system or subsystem and then determine the frequency and impact of the failure. The main objective is to generate a Risk Priority Number (RPN) for each failure mode. The higher the RPN, the more serious the failure could be. Therefore special attention must be paid to the failure mode. FMEA technique is explained in Korayem and Iravani (2008) and two examples of industrial robots (3 linear joints and 6 rotational joints) are analysed and their RPN are calculated.

Carrying out a FMEA requires an initial functional analysis. This functional analysis will depend on the desired degree of precision which will be linked with the size of the subsystems selected, a detailed study can be found in Korayem and Iravani (2008). Thus from the very high level, a robot manipulator can be decomposed into two subsystems:

- a controller subsystem including a computer, microcontrollers, communication links, electronic boards, power suppliers
- an arm which can be decomposed, in its turn, in three subystems:
  - mechanical subsystem including links, joints, gears
  - actuator subsystems including motors, brakes
  - sensors including optical encoders, limit switches.

To illustrate the FMEA procedure an example is given, so all the data concerning the actuator subsystem are listed in Table 1. All the subsystems must be analysed and listed in the same way.

Based on experimental data, each component failure is reviewed, as well as its effect. Its detection is also studied. Each failure is, thus associated with a frequency index, a severity index and a detectability index, with a given range value comprised between 1 and 4.

The RPN is defined as the product of these three indices. Components may then be ranked in decreasing order of criticality. A critical threshold may be set generally speaking on an experimental basis. When the RPN linked to some parts of the robot exceeds the threshold, these parts are sensible and will have to be given a specific attention or be improved. This FMEA is essential as far as maintenance plans have to be defined. It is also fundamental in the understanding of failures that can occur on the robot. In the field of fault tolerance, it has to be completed by a dynamic study of the faulty robot for a better understanding of the robot motion with faults. A dynamic study will also provide information on the indicators to be defined for the detection stage. The dynamic model of the robot has to be established and this is the aim of the following section.

3 State space model and fault analysis

3.1 Modelling-actuation scheme

The considered robot has five degrees of freedom and all joints are rotational (articulated arms). The dynamic model is based on the Lagrange dynamic equations and describes the voltage required to cause the motion.

Table 1 FMEA-Actuator subsystem

Failure Mode and Effects Analysis (FMEA)

Evaluation	O: Occurence S: Severity D: Detection $RPN = OSD$	Value	1: Very low or none 2: Low or minor 3: Moderate or medium 4: High

System: Robot manipulator 'Sirts'

							Evaluation			
Component	*Function*	*Characteristics*	*Failure mode*	*Causes*	*Local effects (arm)*	*Global effects (robot)*	*O*	*S*	*D*	*RPN*
Actuator subsystem										
Motor	Provides torque	Direct current and permanent magnet	Loss of function	Power supply off, short circuit, shaft break	Stillness	Unaccomplished task	1	2	2	4
			Deterioration of function	Overvoltage, overcurrent, wear-out, greasing, shaft geometrical defect	Velocity and position distorsion, vibrations	Velocity and position alteration, vibrations	2	2	2	8
			Inopportune function	Mechanical overload	Random motion	Unaccomplished task	1	2	2	4
Brake	Brakes shaft 2 and 3 to immobilise the joint	Active when electrical power is interrupted	Loss of function	Complete characteristics loss, wrong programmation	Failing down	Security non assured	1	3	2	6
			Deterioration of function	Characteristics loss	Bad braking	Security non assured	2	3	2	12
			Inappropriate function	Wrong programmation	Locked	Unaccomplished task	1	3	2	6

The initial position is defined in Figure 2.

Figure 2 Initial position of the robot

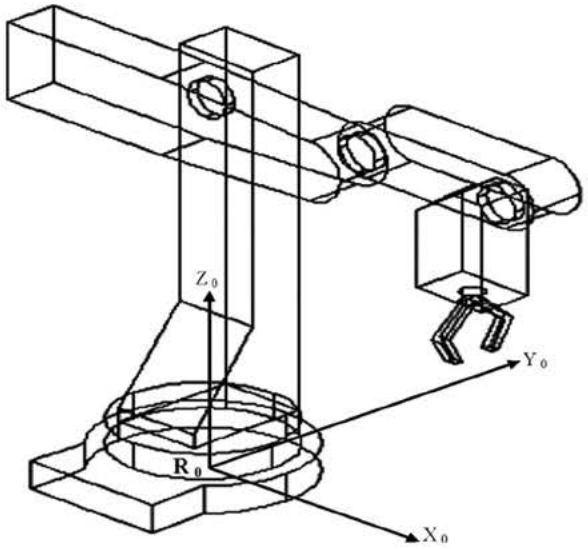

The dynamic model can be expressed as

$$\Gamma = H(\theta)\theta + C(\theta, \dot{\theta})\dot{\theta} + g(\theta),$$

where

$\Gamma \in \mathbb{R}^5$: Generalised joint torque vector
$H(\theta) \in \mathbb{R}^{5\times5}$: Inertia matrix
$\ddot{\theta}, \dot{\theta}, \theta \in \mathbb{R}^5$: Joint angular acceleration, joint angular velocity and joint angular position respectively
$C(\theta, \dot{\theta})\dot{\theta} \in \mathbb{R}^5$: Coriolis and Centripetal forces
$g(\theta) \in \mathbb{R}^5$: Vector of gravity forces.

The actuator of each joint is a DC motor (permanent magnet motor). These motors are equipped with gears and brakes for joints 2 and 3. Once the dynamic model is obtained, the fundamental law of dynamics taking into account the viscous friction, the gear ratio and the motor inertia, leads to obtain

$$\Gamma_m = I_a\ddot{\theta} + F_v\dot{\theta}_m + F_s\text{sgn}(\dot{\theta}_m) + N^{-1}\Gamma,$$

where

$\Gamma_m \in \mathbb{R}^5$: Vector of the motor torque
$I_a = \text{diag}\{I_{a_5}\}$: Diagonal matrix of the actuators inertia
$\ddot{\theta}_m, \dot{\theta}_m \in \mathbb{R}^5$: Actuator angular acceleration, and actuator angular velocity respectively
$F_v = \text{diag}\{F_{v_5}\}$: Diagonal matrix of the viscous friction parameters
$F_s = \text{diag}\{F_{s_5}\}$: Diagonal matrix of the Coulomb friction parameters
$N = \text{diag}\{N_5\}$: Diagonal matrix of the gear ratio parameters.

Thanks to the gear ratio it can be deduced for each joint $\dot{\theta}_m = N\dot{\theta}$. Moreover the motor torque is calculated according to $\Gamma_m = K_{c_i} K_5 v$, where

$K_c = \text{diag}\{K_{c_5}\}$: Diagonal matrix of the motor torque constant parameters
$K = \text{diag}\{K_5\}$: Diagonal matrix of the current amplifier gain parameters
$v \in \mathbb{R}^5$: Vector of the motors input voltage.

Substituting Γ, $\ddot{q}_m$ and $\dot{q}_m$ into Γ_m yields

$$NK_cKv = (I_aN^2 + H(q))\ddot{\theta} + (N^2F_v + C(\theta, \dot{\theta}))\dot{\theta} + g(\theta). \tag{1}$$

It can be deduced

$$\begin{aligned}\ddot{\theta} = &-(I_aN^2 + H(\theta))^{-1}(N^2F_v + C(\theta, \dot{\theta}))\dot{\theta} + (I_aN^2 + H(\theta))^{-1}NK_cKv \\ &- (I_aN^2 + H(\theta))^{-1}g(\theta).\end{aligned} \tag{2}$$

Let us introduce the state vector $x \in \mathbb{R}^{10} : x = [x_1\ x_2]^T = [\theta_1\ \cdots\ \theta_5\ \dot{\theta}_1\ \cdots \dot{\theta}_5]^T$.

Substituting x into equation (2) yields

$$\begin{cases}\dot{x}_1 = x_2 \\ \dot{x}_2 = -A(\theta, \dot{\theta})x_1 + B(\theta)v - G(\theta)\end{cases},$$

where $A(\theta, \dot{\theta}) \in \mathbb{R}^{5\times5}$, $B(\theta) \in \mathbb{R}^{5\times5}$ and $G(\theta) \in \mathbb{R}^5$ with

$$\begin{aligned}A(\theta, \dot{\theta}) &= (I_aN^2 + H(\theta))^{-1}(N^2F_v + C(\theta, \dot{\theta})) \\ B(\theta) &= (I_aN^2 + H(\theta))^{-1}NK_cK \\ G(\theta) &= (I_aN^2 + H(\theta))^{-1}g(\theta).\end{aligned}$$

Only the position is measured, so the state space model is defined as, equation (3)

$$\begin{cases}\dot{x} = \begin{bmatrix}0 & 1 \\ 0 & -A(\theta, \dot{\theta})\end{bmatrix}x + \begin{bmatrix}0_{(5*5)} \\ B(\theta)\end{bmatrix}v + \begin{bmatrix}0_{(5\times1)} \\ -G(\theta)\end{bmatrix}. \\ y = Cx = [I_{(5\times5)}\ \ 0_{(5\times5)}]x\end{cases} \tag{3}$$

The parameters in the robot manipulator dynamic model used are of two different types:

- *Electrical parameters*: v, K
- *Mechanical and electromechanical parameters*: I_a, F_v, F_s, N, K_c, H, C, and g.

By solving equation (3), it is possible for us to simulate several fault types by modifying the associated parameters and to observe all consequences on the robot trajectories. A detailed study of many possible faults is given in Noureddine (1996), in which a study of both position and velocity of the robot in function of some parameters evolution such as dry friction, is presented.

To be concise, we present in this work the study of two faults, the first one is an increase in the dry coefficient of joint 2 to illustrate the dynamic analysis. The second one deals with the actuator of joint 3 and will be used to illustrate the fault detection algorithm followed by the fault accommodation stage.

3.2 *Fault dynamic analysis*

Using equation (2), angular position and velocity are determined at $t = 5$ s. All voltages are referenced to zero, so arm 1 is not subject to any force and will therefore not move. As opposed to that, arms 2 and 3 are submitted to the gravity forces and reach an equilibrium in a vertical position as shown in continuous line in Figure 3. For clarity reasons, arms 3 and 4 have not been represented.

Figure 3 Normal and faulty trajectories

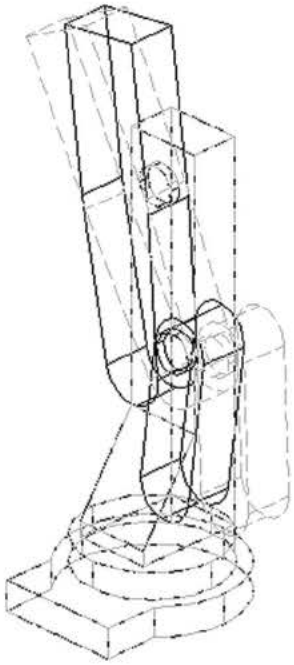

What would happen, at still $t = 5$ s, if a fault occurred in the system while the inputs remained unchanged (= all voltage references to zero)?

Let us study, for example, the influence of a high increase in the dry coefficient of joint 2 (100 times higher than the nominal value). As a consequence, it is clear that the motion of arm 2 will decrease and that, at $t = 5$ s, the amplitude of the motion will not be as wide as in the normal case. This is shown in Figure 3 where the robot, in this case, is drawn in broken line.

3.3 *Fault modelling*

Most FDI works assimilate the faults to additive terms in the state equation when the model with faults has to be designed. This term is added to the dynamic equation for dynamic faults and another one to the measure equation for the sensor faults. This formulation, if it does not allow the faulty parts of the system to be stressed, has the advantage of keeping the linear properties of the model and permits the application of all linear techniques developed for Linear Time Invariant systems for fault detection and isolation.

In general we have to consider the following two types of faults:

- Sensor faults

The sensor faults will affect the position values given by the optical encoders of each joint. To simulate the occurence of a fault in the position measure, an offset can be generated on the output of the modelled system. A vector of sensor fault (measurement fault) $f_m \in \mathbb{R}^5$ multiplied by a fault distribution matrix $K_m = \text{diag}\{K_{m_5}\}$ is defined in the output equation of the state space model

$$y = Cx + K_m f_m,$$

where $f_m = [f_{m1}\ f_{m2}\ f_{m3}\ f_{m4}\ f_{m5}]^T$. This type of fault is not taken into account in the FDI and fault accommodation stages.

- Dynamic faults

Dynamic faults occur on the mechanical part of the robot, on the actuators and on the electronic interfaces. This type of fault will appear in the dynamic equation of the system as a vector $f_d \in \mathbb{R}^5$ multiplied by a fault distribution matrix $K_d = \text{diag}\{K_{d_5}\}$,

$$\dot{x} = \begin{bmatrix} 0 & 1 \\ 0 & -A(\theta, \dot{\theta}) \end{bmatrix} x + \begin{bmatrix} 0_{(5\times5)} \\ B(\theta) \end{bmatrix} v + \begin{bmatrix} 0_{(5\times1)} \\ -G(\theta) \end{bmatrix} + \begin{bmatrix} 0_{(5\times5)} \\ K_d \end{bmatrix} f_d, \tag{4}$$

where $f_d = [f_{d1}\ f_{d2}\ f_{d3}\ f_{d4}\ f_{d5}]^T$.

We consider only one dynamic fault, it is indeed sufficient enough to illustrate the fault accommodation algorithms and it simplifies the FDI stage very much. The dynamic fault concerns joint 3 and more precisely the motor 3 servoamplifier. The actuators and their associated electronic interfaces are main parts in mechatronic systems and some works still deal with them (Wang and Daley, 1996). Fault simulation has been achieved by considering a short circuit which induces a low or high saturation of the output of some operational amplifiers.

It is obvious that these types of faults can occur on any joint but the whole development of the FDI stage is not the purpose of this paper. Due to this restrictive hypothesis we can deduce: $f_d = [0\ 0\ f_{d3}\ 0\ 0]^T$ and the isolation problem is not dealt with.

4 State space control and fault detection

The FDI algorithms are very closely linked to the control algorithms. For the control, several methods are usually used and especially the exact linearisation through state feedback, named computer torque method in the joint space, when the aim is control tracking. When the objective is point to point motion, a local linearisation is possible around a fixed point. In this paper the specified task given to the robot belongs to this category.

4.1 *Operating point*

The operating point fixed in our application is defined by the vector of the end-effector position $P = (P_x\ P_y\ P_z)$ which sets the end-effector coordinates in the frame R_0, (see Figure 4) with $P_x = 0.30\,\text{m}$, $P_y = 0$, $P_z = 0.80\,\text{m}$. The end-effector orientation is imposed by two angles, the pitch angle: $\theta_{234} = 10°$, $(\theta_{234} = \theta_2 + \theta_3 + \theta_4)$ and the yaw angle: $\theta_5 = 0°$.

Figure 4 Denavit-Hartenberg frames

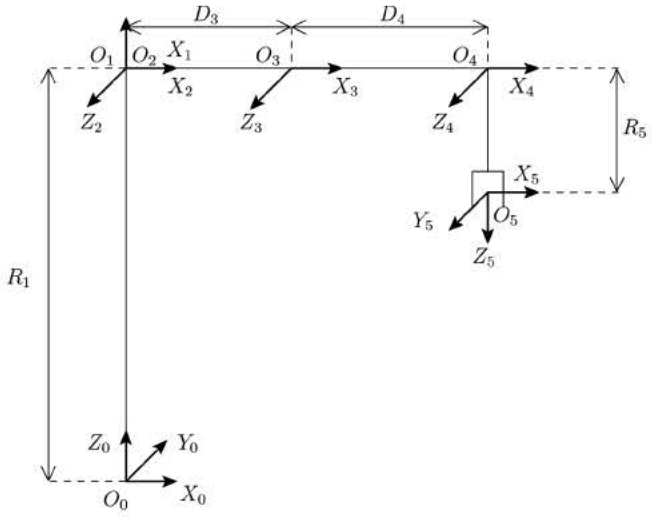

The vector of joint variables is achieved thanks to the inverse kinematic model. When the desired position and orientation of the end-effector are given, this model permits the computation of a set of joint angles which will obtain the desired position of the end-effector. The equations are written thanks to the Denavit-Hartenberg formalism (Craig, 1989), where R_1, D_3, D_4 and R_5 are the lengths of the arms defined in Figure 4.

θ_1 is obtained from the first equation of the inverse kinematic model

$$P_x \sin\theta_1 - P_y \cos\theta_1 = 0, \quad \text{so } \theta_1 = \text{arctg}\left(\frac{Py}{Pz}\right).$$

The angle θ_3 is calculated by

$$\theta_3 = \arccos\left(\frac{A}{B}\right)$$

with

$$\begin{aligned} A &= (Z_2)^2 + (Z_1)^2 - (D_3)^2 - (D_4)^2 \\ B &= 2D_3D_4 \\ Z_1 &= P_z - R_1 + R_5 \cos\theta_{234} \\ Z_2 &= P_x \cos(q_1) + P_y \sin(\theta_1) - R_5 \sin\theta_{234}. \end{aligned}$$

According to the signs of the variables A and B, θ_3 will be obtained by two possible solutions and only the positive value will be held.

Then θ_2 is obtained by

$$\sin\theta_2 = \frac{Z_1B_1 - Z_2B_2}{(B_2)^2 + (B_1)^2}, \quad \cos\theta_2 = \frac{Z_1B_2 + Z_2B_1}{(B_2)^2 + (B_1)^2} \quad \text{so } \theta_2 = \arctan\left(\frac{\sin\theta_2}{\cos\theta_2}\right),$$

with

$$B_1 = D_3 + D_4\cos\theta_3, \quad B_2 = D_4\sin\theta_3$$

θ_4 is deduced thanks to θ_{234} which is a given value defined by the imposed orientation.

$$\theta_4 = \theta_{234} - \theta_2 - \theta_3.$$

The vector of the joint, relative to the chosen fixed point, is finally obtained, (see Figure 5).

$$\theta_e = (\theta_1\ \theta_2\ \theta_3\ \theta_4\ \theta_5)^T = (60^\circ\ -4^\circ\ 45^\circ\ -31^\circ\ 0^\circ)^T.$$

Figure 5 Operating point in faultfree mode

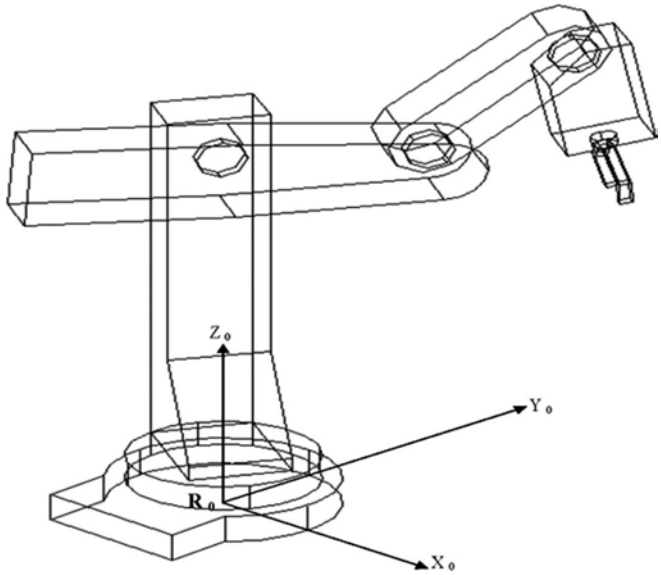

4.2 Local linearisation and state space control

The robot is dedicated to operate around a fixed point which is an equilibrium point $E = (y_e, x_e, v_e)$. A local linearisation around this point will be achieved. $\Phi(\dot{x}, x, v)$ and $\Psi(y, x, v)$ are written

$$\begin{cases} \Phi = \begin{bmatrix} \dot{x}_1 - x_2 \\ \dot{x}_2 + A(\theta, \dot{\theta})x_2 - B(\theta)v + G(\theta) \end{bmatrix} = 0 \\ \Psi = y - x_1 = 0 \end{cases}. \tag{5}$$

Let us define the following variables:

$$\tilde{x} = \begin{pmatrix} \tilde{x}_1 \\ \tilde{x}_2 \end{pmatrix} = \begin{pmatrix} x_1 - x_{e_1} \\ x_2 - x_{e_2} \end{pmatrix}, \quad \tilde{y} = y - y_e$$

and $\tilde{v} = v - v_e$ where y_e and v_e are respectively the output vector and the input voltage vector at the equilibrium point. The latter is obtained by substituting $\ddot{\theta}_i = \dot{\theta}_i = 0$ into equation (1), thus: $v_e = [NK_cK]^{-1}g(\theta)$ which leads to $v_e = (v_{1_e}\ v_{2_e}\ v_{3_e}\ v_{4_e}\ v_{5_e})^T$.

The linear model is obtained by

$$\dot{\tilde{x}} = A_{\text{lin}}\tilde{x}(t) + B_{\text{lin}}\tilde{v}(t) \quad \tilde{y}(t) = C_{\text{lin}}\tilde{x}(t) \tag{6}$$

with

$$A_{\text{lin}} = -\left[\frac{\partial \Phi(\dot{x}, x, v)}{\partial \dot{x}}\bigg|_E\right]^{-1} \frac{\partial \Phi(\dot{x}, x, u)}{\partial x}\bigg|_E$$

$$B_{\text{lin}} = -\left[\frac{\partial \Phi(\dot{x}, x, u)}{\partial \dot{x}}\bigg|_E\right]^{-1} \frac{\partial \Phi(\dot{x}, x, u)}{\partial u}\bigg|_E$$

$$C_{\text{lin}} = -\left[\frac{\partial \Psi(\dot{x}, x, u)}{\partial \dot{x}}\bigg|_E\right]^{-1} \frac{\partial \Psi(\dot{x}, x, u)}{\partial x}\bigg|_E.$$

where Φ and Ψ are given in equation (5).

To obtain a position error which leads assymptotically to zero, a well-known state feedback is designed. The closed-loop poles are defined by a pole placement design method. First, the controllability-canonical form of equation (6) is achieved.

A proportional state space controller enables one to define : $v = v_e - K_v\tilde{x}_2 - K_p\tilde{x}_1$ where K_v and $K_p \in \mathbb{R}^{5\times 5}$ and represent the state feedback gain.

Only the angular position vector x_1 is measured and thus it is necessary to estimate the angular velocity vector x_2. The gain matrix of the observer is obtained from the observability canonical form. For the stability of the observer and in order that the error converges to zero very fast, the observer poles have been chosen sufficiently negative.

4.3 Fault detection

The residual generation using observers is one of the main model based methods. A large number of surveys can be found in the literature and describe all the possibilities and performances of these techniques, especially in Garcia and Franck (1997).

It has been necessary to estimate the joint velocities in the control stage. Instead of designing a reduced observer to determine only the joint velocities, a full order observer has been designed to obtain redundant information as the joint positions. Thus an indicator, named residual, based on the comparison between estimated and measured position is constructed such that

$$r(t) = \theta(t) - \hat{\tilde{\theta}}(t).$$

The residual $r(t)$ takes a significant value if a fault occurs while it remains close to zero without faults. The control architecture including the detection stage is described in Figure 6.

Figure 6 Control and detection scheme

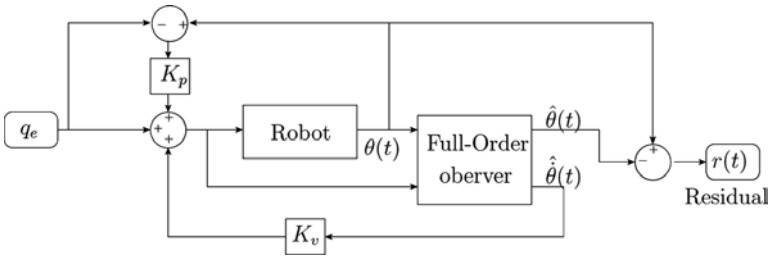

4.3.1 Simulation

As mentioned in Section 3.3, a saturation at +5V is implemented at $t = 3\,\mathrm{s}$. A significant residual value is then deduced which expresses the fault occurence, (see Figure 7). The residual has also a non-negligible value during the end-effector motion. This value is due to the fact that the model does not match the one established around the operating point. This phase lasts about 0.75 s. From 0.75 s to 3 s, the residual $r(t)$ is almost nil due to a normal mode.

Figure 7 Simulation results

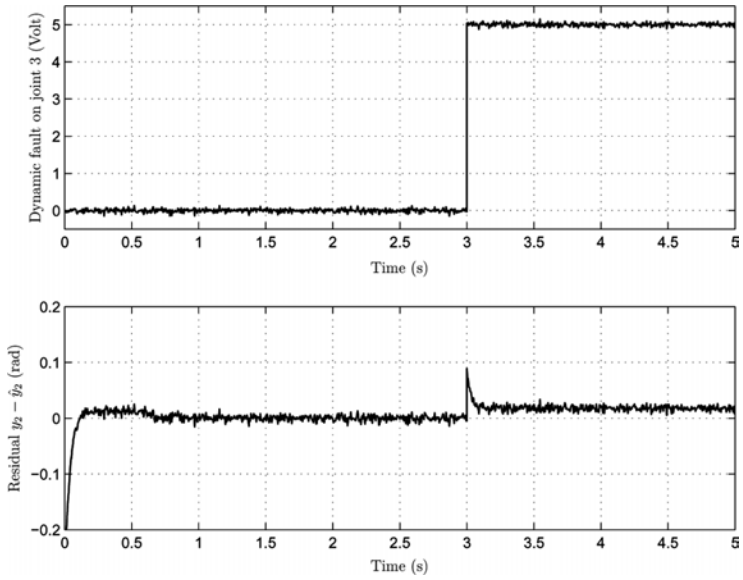

A decision stage, which can be applied in the case where the signals are little noisy, is made by thresholding the residual $r(t)$. Let us remember that this detection is highly facilitated by the fact that only faults on joint 3 are taken into account. The problem will be more complicated if all possible faults on the 5 joints are considered, and in particular the problem of locating the fault. A scheme composed of observers coupled with some unknown input observers are generally necessary to obtain structural residuals and allow fault detection and isolation (Patton and Chen, 1997).

5 Fault accommodation

Due to their mechanical structure, some robots can have the advantage of being kinematically redundant. In the general case, the position and the orientation of the end-effector within the workspace necessitates six degrees of freedom. For example, any kinematic redundancy would require a seventh joint. For the robot in question and although it has only 5 joints, that is to say limited in its orientation, the mechanical structure implies that joints 2–4 are moving in the same plan, thus creating a redundancy for the positioning of the end-effector. This structural redundancy can be implemented to create fault tolerant algorithms which could be used to provide alternative configurations in failure situations. This redundancy has the great advantage of not requiring any supplementary joint and thus not complexifying the mechanical structure as described in Groom et al. (1999), Chen et al. (2003) and English and Maciejewski (2000). It is well known that the more mechanical components we add, the more we fragilise the whole system. In the same way, any failure of the robot joint can lead to both a loss of accessibility in the task space or a loss of orientation capability, but a trajectory reconfiguration will enable a working in a more limited form. Any robot manipulator can have some redundancy capability for a given task. In order to study these capabilities it is very important to identify the workspace of the robot. This workspace is a given specification by

$$\begin{aligned} 0^\circ < \theta_1 < 180^\circ \\ -15^\circ < \theta_2 < 80^\circ \\ -105^\circ < \theta_3 < 105^\circ \\ -35^\circ < \theta_4 < 195^\circ \\ -360^\circ < \theta_5 < 360^\circ. \end{aligned} \tag{7}$$

The calculus methods of the direct and inverse geometric models require to associate benchmarks for each axis, according to specific conventions described in the robotics literature. The calculus of the geometric model enables to set the degrees in the operational space through the variation of the angular position of the robot given in equation (7). A perspective representation, given in Figure 8 shows the reachable volume characterised by the equation (8).

$$\begin{cases} s_x = \cos\theta_1 \cos\theta_{234} \cos\theta_5 + \sin\theta_1 \sin\theta_5 \\ s_y = \sin\theta_1 \cos\theta_{234} \cos\theta_5 - \cos\theta_1 \sin\theta_5 \\ s_z = \sin\theta_{234} \cos\theta_5 \\ n_x = -\cos\theta_1 \cos\theta_{234} \sin\theta_5 + \sin\theta_1 \cos\theta_5 \\ n_y = -\sin\theta_1 \cos\theta_{234} \sin\theta_5 - \cos\theta_1 \cos\theta_5 \\ n_z = -\sin\theta_{234} \sin\theta_5 \\ a_x = \sin\theta_{234} \cos\theta_1 \\ a_y = \sin\theta_{234} \sin\theta_1 \\ a_z = -\cos\theta_{234} \\ P_x = R_5 \cos\theta_1 \sin\theta_{234} + \cos\theta_1 (D_3 \cos\theta_2 + D_4 \cos\theta_{23}) \\ P_y = R_5 \sin\theta_1 \sin\theta_{234} + \sin\theta_1 (D_3 \cos\theta_2 + D_4 \cos\theta_{23}) \\ P_z = -R_5 \cos\theta_{234} + D_3 \sin\theta_2 + D_4 \sin\theta_{23} + R_1 \end{cases} . \tag{8}$$

Figure 8 Robot workspace

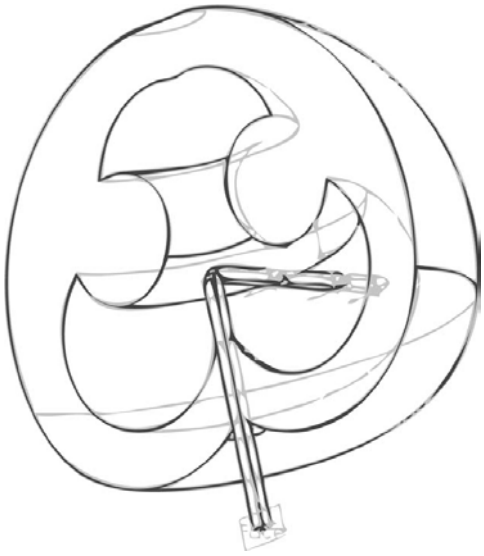

5.1 Failure of joint 3

To illustrate the fault accommodation procedure, joint 3 is considered locked in its initial position. In an industrial context, it is generally thought that this arm can be repositioned in its original position whatever fault might have occurred and whatever position the arm might have been locked in. The new and reduced workspace corresponds to a joint situation where joint 3 is maintained to 0. To calculate the alternative joint configuration which should permit the operating point to be reached, we had to calculate once again the inverse kinematic model with $\theta_3 = 0$. Let's remember that the operating point is given by a position specified by $P_x = 0.30\,\text{m}$, $P_y = 0$, $P_z = 0.80\,\text{m}$ and an orientation specified by $\theta_{24} = 10^\circ$ and $\theta_5 = 0^\circ$. The angles are given by

$$\theta_1 = \text{arctg}\frac{P_y}{P_x} = 60^\circ.$$

$$\theta_2 = \text{arctg}\frac{\sin\theta_2}{\cos\theta_2} \quad \text{with} \quad \sin\theta_2 = \frac{B_2}{D_3 + D_4} \quad \text{and} \quad \cos\theta_2 = \frac{B_4}{B_3}$$

where

$$B_2 = P_z - R_1 + R_5\cos\theta_{24}$$
$$B_3 = (D_3 + D_4)\cos\theta_1$$
$$B_4 = P_x - R_5\cos\theta_1\sin\theta_{24} - D_3$$

and finally $\theta_2 = 18^\circ$ θ_4 is obtained by $\theta_4 = \theta_{24} - \theta_2 = -8^\circ$.

The alternative joint configuration is $\theta = (\theta_1\ \theta_2\ \theta_3\ \theta_4\ \theta_5)^T = (60^\circ\ 18^\circ\ 0^\circ\ -8^\circ\ 0^\circ)^T$ and shown in Figure 9.

Figure 9 Redundant joint configuration

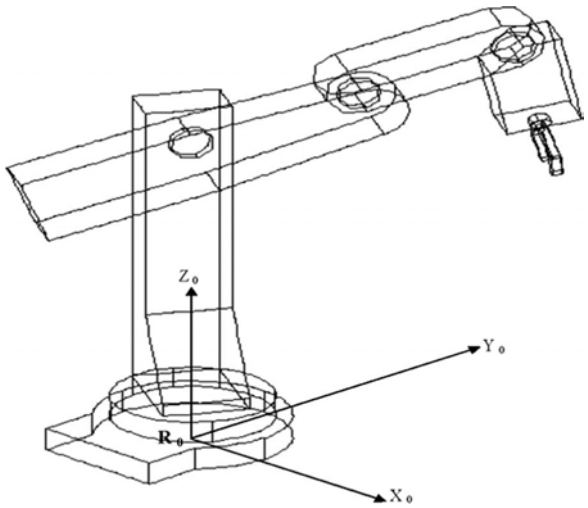

6 Conclusion

Each and every step for designing a fault tolerant robot manipulator has been proposed. Some steps have been implemented on the real robot whereas the fault introduction and fault detection stages have been simulated. The results of the analysis phase have shown a criticity scale of all the robot components. These results are useful not only for the design of a fault tolerant system but also when a plan of maintenance is defined. The FDI algorithms have been simplified due to the fact that only one fault has been considered and the problem of isolation is not adressed in this work.

The calculation of the inverse kinematic model, under condition of fault on joint 3, permits the generation of an alternative operating point. This reconfiguration has been made possible thanks to the mechanical structure of the considered robot.

References

Chen, Y., McInroy, J. and Yi, Y. (2003) 'Optimal, fault-tolerant mappings to achieve secondary goals without compromising primary performance', *IEEE Trans. Robotics and Automation*, Vol. 19, No. 4, pp.680–691.

Chow, E. and Willsky, A. (1984) 'Analytical redundancy and the design of robust failure detection systems', *IEEE Trans. Automatic Control*, Vol. 233, No. 7, pp.650–614.

Craig, J. (1989) *Introduction to Robotics*, 2nd ed., Addison-Wesley, New York.

English, J. and Maciejewski, A. (2000) 'Measuring and reducing the euclidean-space effects of robotics joint failures', *IEEE Trans. Robotics and Automation*, Vol. 16, No. 1, pp.20–28.

Garcia, E. and Franck, P. (1997) 'Deterministic non linear observer-based approaches to fault diagnosis: a survey', *Control Eng. Practice*, Vol. 5, No. 5, pp.663–670.

Groom, K., Maciejewski, A. and Balakrishnan, V. (1999) 'Real-time failure-tolerant control of kinematically redundant manipulators', *IEEE Trans. Robotics and Automation*, Vol. 15, No. 6, pp.1109–1116.

Hassan, M. and Notash, L. (2007) 'Optimizing fault tolerance to joint jam in the design of parallel robot manipulators', *Mechanism and Machine Theory*, Vol. 42, pp.1401–1417.

Isermann, R. (1997) 'Supervision, fault detection and fault-diagnosis methods-an introduction', *Control Eng. Practice*, Vol. 5, No. 5, pp.639–652.

Korayem, M. and Iravani, A. (2008) 'Improvement of 3p and 6r mechanical robots reliability and quality applying FMEA and QFD approaches', *Robotics and Computer-Integrated Manufacturing*, Vol. 24, pp.472–487.

Noureddine, F. (1996) 'Conception d'un outil logiciel graphique pour l'analyse comportementale d'un robot en mode dgrad', *Revue Internationale de CFAO et d'Informatique Graphique, Hermes Edition*, Vol. 11, pp.199–214.

Paredis, C., Au, W. and Khosla, P. (1994) 'Dexterity optimization of kinematically redundant manipulators in the presence of joint failures', *Computers and Electrical Engineering*, Vol. 20, No. 3, pp.273–288.

Patton, R. and Chen, J. (1997) 'Observer-based fault detection and isolation: robustness and applications', *Control Eng. Practice*, Vol. 5, No. 5, pp.639–652.

Sarkar, N., Podder, T. and Antonelli, G. (2002) 'Fault-accommodating thruster force allocation of an auv considering thruster redundancy and saturation', *IEEE Trans. Robotics and Automation*, Vol. 18, No. 2, pp.223–233.

Visinsky, M., Cavallaro, J. and Walker, I. (1994) 'Robotic fault detection and fault tolerance: a survey', *Reliability Engineering and System Safety*, Vol. 46, pp.139–158.

Visinsky, M., Cavallaro, J. and Walker, I. (1995) 'A dynamic fault tolerance framework for remote robots', *IEEE Trans. Robotics and Automation*, Vol. 11, No. 4, pp.477–489.

Wang, H. and Daley, S. (1996) 'Actuator fault diagnosis: an adaptive observer-based technique', *IEEE Trans. Automatic Control*, Vol. 41, No. 7, pp.1073–1078.

Yang, J. (2008) 'Omnidirectional walking of legged robots with a failed leg', *Mathematical and Computer Modelling*, Vol. 47, pp.1372–1388.